

Metal-Loaded Mesoporus Materials for Production of Dimethyl Carbonate

Ahmed Arafat, Yahia Alhamed and Abdul Rahim Al-Zahrani

Chemical & Materials Engineering Department, College of Engineering, King Abdulaziz University, P.O. Box 80204 Jeddah 21589, E-mail: akhamis@kau.edu.sa

Abstract:

Relatively high yields of dimethylcarbonate (DMC) are obtained by reaction of carbon dioxide and methanol using ceria or zirconia-loaded mesoporous TUD-1 catalysts. Series of mesoporous TUD-1 catalysts loaded with different ratios of ceria, zirconia and mixture of these oxides were prepared directly by hydrothermal methods. Catalyst samples were characterized by x-ray diffraction (XRD), UV-Vis spectroscopy and scanning electron microscopy (SEM). Catalytic testing showed a better performance of TUD-1 loaded with mixed ceria and zirconia. However, relatively high DMC yields were obtained via introduction of dehydrating agents in the reaction mixture in addition to the catalyst.

Introduction:

Recently, dimethylcarbonate (DMC) has drawn much attention in phasing out environmentally unfriendly compounds in fuels. This is concluded by the large number of patents and research papers on the production and application of this material in the last two decades.[1] Conventionally, synthesis of DMC

Nevertheless, oxidative carbonylation of methanol has been recently pursued over a variety of catalysts as an “environmentally friendly” nonphosgene production pathway to DMC:



Previous investigations described new reaction routes, variety of catalysts as well as studies on the mechanism of the reaction pathway involved in the vapor-phase carbonylation of methanol to DMC over copper zeolite catalysts.[2,3] However, preparation of DMC by direct reaction of methanol and carbon dioxide still problematic due to the need of efficient catalysts, the methylating effect of DMC itself and the sensitivity of reaction to the formation of minute amounts of water.[4-7] therefore, an efficient, selective catalyst is needed for better production of this material, in this context, functionalized-TUD-1, 3-D mesoporus catalyst can be a good candidate for this process.

This paper includes preparation, characterization and testing of metal oxide-loaded mesoporous catalysts for preparation of dimethylcarbonate (DMC) through the reaction between methanol and carbondioxide employing a 3-D mesoporus TUD-1 catalysts loaded with ceria, zirconia and or a mixture of ceria and zirconia.

Experimental

Preparation of metal-loaded TUD-1 Catalysts

Ce-TUD-1 was prepared following a modified procedure for the all-silica material TUD-1.[8] R-Ce(acac)₄ was used as the cerium precursor and was prepared according to Behrsing et al.[9] Four samples of Ce-TUD-1 have been prepared in which the Si/Ce is varied as 10, 25, 50 and 100.

Synthesis of Zr-TUD-1

Zr-TUD-1 was synthesized with triethanolamine (TEA) as chelating agent in a one-pot procedure based on the sol-gel technique. [10] Samples with a Si to Zr ratio of 100, 50, 25 and 10 (denoted as Zr-TUD-1 (100), Zr-TUD-1(50), Zr-TUD-1(25) and Zr-TUD-1(10), respectively) were prepared.

Characterization of the prepared catalysts

XRD. Powder X-ray diffraction patterns were measured on a Philips PW 1840 diffractometer. The samples were scanned over a range of 0.1-80° 2θ with steps of 0.02°.

N₂ adsorption. Nitrogen adsorption/desorption isotherms were recorded on a QuantaChrome NOVA 2200e at 77 K. The pore size distribution was calculated from the adsorption branch using the Barret-Joyner-Halenda (BJH) model [11]. Samples were previously evacuated at 623 K for 16 h. The BET method was used to calculate the surface area (S_{BET}) of the samples, while the mesopore volume (V_{meso}) was determined with the t-plot method according to Lippens and de Boer[12].

SEM. Scanning Electron Microscopy images were recorded at 10kV on a Philips XL 20 microscope. Samples coated with gold to avoid charging effects and to enhance contrast.

UV-Vis. The materials prepared were investigated by diffuse reflectance UV-Vis spectroscopy. Spectra were collected at ambient temperature on a CaryWin 300 spectrometer using BaSO₄ as reference.

Catalytic Tests:

The reaction was carried out in a stainless steel autoclave reactor with an inner volume of 2 L. The standard procedure is as follows: 610 g CH₃OH (Across) and 5 g catalyst were put into an autoclave, and then the reactor was purged with CO₂. After that, the autoclave was pressurized with CO (AHG). The reactor was heated and magnetically stirred constantly during the reaction.

Reactant chemicals and CO₂ were used without further purification. The total pressure at 383 K was about 6 MPa (200 mmol CO₂). After the reaction, the gas was collected in a gas bag. Products in both the gas and liquid phases were analyzed with a gas chromatograph (GC) equipped with FID and TCD. The separation column packing is TC-WAX for FID-GC and Porapak N for TCD-GC.

Results and Discussions

Synthesis of mesoporous Ce-TUD-1 catalysts:

Synthesis of Ce-TUD-1 was carried out in presence of acetylacetonate complex of Ce(IV) which known to have good solubility in ethanol, thus making it miscible with TEOS and triethanol amine, and because its decomposition after the addition of water is slow. Figure 1 depicts the X- ray diffraction patterns of the obtained Ce-TUD-1 samples.

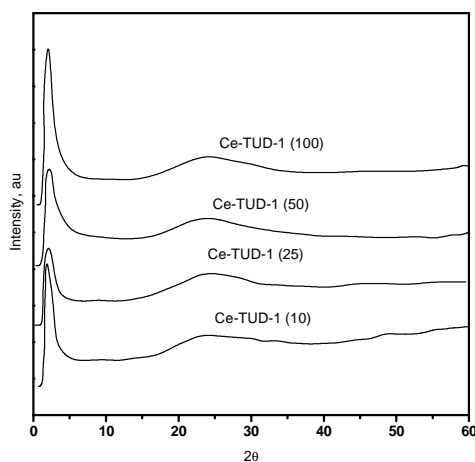


Figure 1. X-ray diffraction patterns of Ce-TUD-1 samples

All samples show a single intense peak at $1-2.5^\circ 2\theta$, which corresponds to a short-range correlation of nuclear density at a distance of 45-47 Å. The peak is instrument-limited on the small-angle side, but with increasing metal content it weakens, broadens, and shifts to larger angles. This implies that the short-range order is increasingly disrupted, and that the remaining structures are smaller and more heterogeneous. This indicates that Ce-TUD-1 is a non-crystalline, meso-structured material. The intensity of the peak decreases with increasing metal loading as a result of the influence of metal oxide particles on the integrity of the mesoporous structure. Moreover, XRD patterns showed that the prepared samples are pure, there is no detectable metal oxide phase or other bulky dense phases in the samples.

XRD analysis revealed no peaks at higher angle, which is in accordance with the amorphous nature of the cerium silicate framework and the absence of large CeO_2 crystallites, which would be detected by XRD. The peak associated with pores with a diameter of around 200 Å lies outside the detection range of the instrument ($2\theta > 1^\circ$) and could therefore not be detected.

Figure 2 illustrates the N_2 adsorption/desorption isotherms of metal-loaded TUD-1 samples.

Generally, according to IUPAC classification, the hysteresis loops are characteristic features of type IV isotherms, representative for mesoporous materials [13].

One can distinguish two characteristic types of hysteresis loops. In the first case, (Figure 3) at lower metal loading the loop is relatively narrow, the adsorption and desorption branches being almost vertical and nearly parallel (*H1*), which means that the isotherm is governed by delayed condensation, pores filling and emptying appear to occur in a narrow range on uniform near-cylindrical pores. At higher metal loading the hysteresis loop becomes broad, desorption branch being much steeper than the adsorption one, pores filling and emptying in a wide range on non-uniform pores (*H4*). This behaviour can be explained by the formation of nano-particles of metal oxides inside the pores at higher metal loading.

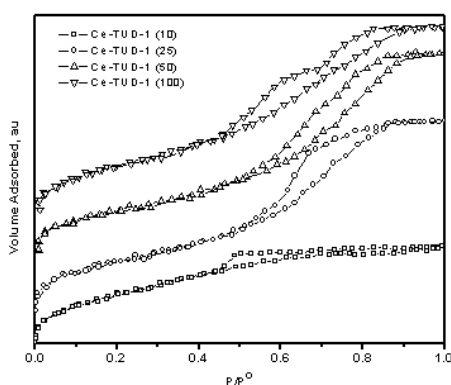


Figure 2. N_2 adsorption isotherms at 77 K recorded for cerium-loaded TUD-1 samples

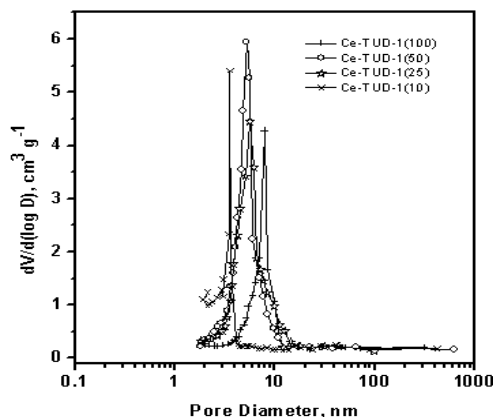


Figure 3. Pore size distribution of cerium-loaded TUD-1 samples obtained from the N_2 adsorption data at 77K.

The pore size distributions of different Ce-TUD-1 samples are shown in Figure 5. It is clear that all the samples show a very narrow pore size distribution in the range from 3-10 nm. The relatively narrower pore size distribution in higher metal loadings is understandable when the formation of cerium oxide nanoparticles is considered.

The N_2 adsorption and elemental analysis of Ce-TUD-1 samples with different Si:Ce ratios, Ce-TUD-1(10), Ce-TUD-1(50), and Ce-TUD-1(100), are presented in Table 2.

Table 1. Porosity and compositional Properties of Ce-TUD-1

Sample	BET Surface area (m ² /g)	Total Pore Volume (mL/g)	Average Pore Diameter (Å)	Si:Ce
Ce-TUD-1(10)	660	1.8	122	11.2
Ce-TUD-1(25)	550	1.72	144	24.8
Ce-TUD-1(50)	430	1.8	205	48.2
Ce-TUD-1(100)	412	1.82	225	95.5

The BET surface areas are around 500 m²/g, the pore size distribution exhibits a maximum at around 200 Å, and the total pore volumes are around 1.80 cm³/g, which is in the same range as TUD-1 samples reported previously.[14]

The UV-Vis spectra of calcined Ce-TUD-1 samples previously preheated at 180 °C for 24 h are presented in Figure 6. Two main peaks around 265 and 350 nm were found in all spectra. This is due to the fact that cerium dioxide strongly absorbs UV light at $\lambda < 400$ nm with an absorption edge at $\lambda = 400$ nm which is reported to blue-shift for CeO₂ crystallite sizes of 1-5 nm. In addition to blue shift, the UV-Vis spectra can detect < 100 ppm of cerium in a powder material and shows narrow band in the range of 250-350 nm for CeO₂ crystallites of < 2 nm. The narrow bands are attributed to localized O-Ce charge transfer transitions involving a number of surface Ce⁴⁺ ions with different coordination numbers [15,16].

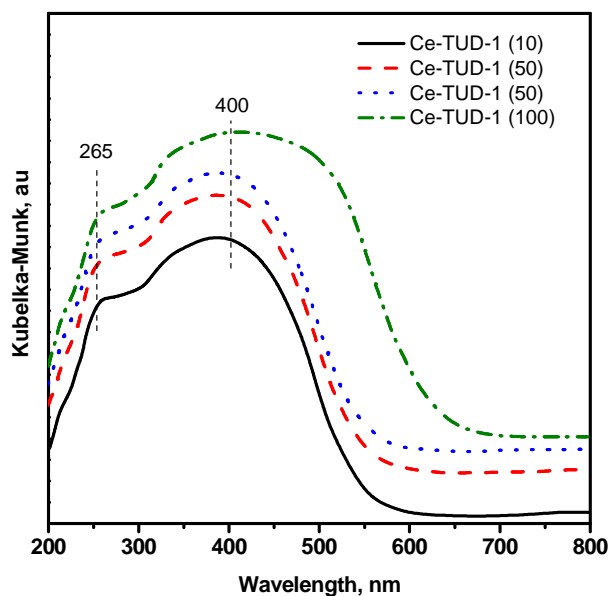


Figure 4. The UV-Vis spectra of Cerium-loaded TUD-1 samples previously heated at 180 °C for 24 h.

Scanning electron micrograph of Ce-TUD-1 materials did not revealed any structural indication of the material. The SEM images of cerium loaded TUD-1 are presented in Figure 5. The image shows that the particles do not have any well-defined morphology. In general, the samples consist of about 40-50 µm irregularly-shaped particles. The SEM image is in line with the images of Au/Ti-TUD-1 sample presented by Haruta et al [17]. However, at high metal loading samples, the metal TUD-1 structure is changed to less uniform structures, than the low metal loading samples. This indicates the influence of a high metal concentration on the TUD-1 structure.

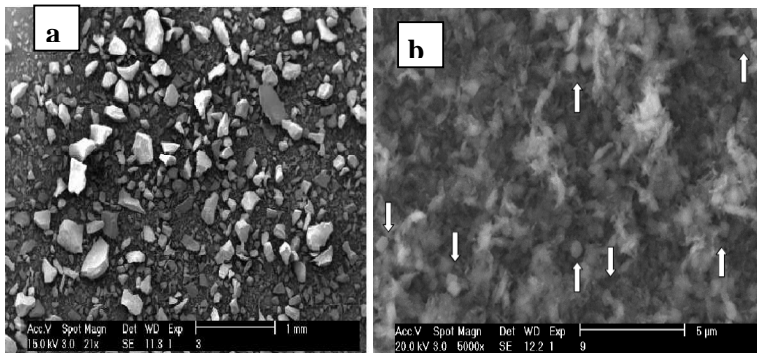


Figure 5. SEM micrograph of Ce-TUD-1 material, (a) Ce-TUD-1 (10) and (b) Ce-TUD-1 (100).

Synthesis of mesoporous Zr-TUD-1 catalysts.

Samples of zirconium-loaded three-dimensional mesoporous TUD-1 catalysts have been prepared by hydrothermal technique. Different Si/Zr ratios have been used in the synthesis mixture to afford catalysts with different activities in the production of dimethyl carbonate via the direct reaction of methanol and carbon dioxide.

XRD analysis of the obtained catalysts are shown in Figure 6.

A broad intense peak at low angle ($0.4\text{--}2\ \theta$) was observed in the X-ray powder diffraction pattern for all calcined Zr-TUD-1 samples (Figure 7) demonstrating the mesostructured character of these materials. No evidence for crystalline ZrO_2 was observed in the X-ray diffractograms, indicating that zirconium is incorporated into the framework. In line with the effects of metal loading in Co-TUD-1[18] and Al-TUD-1,[19] the peak intensity decreases slightly with an increase in the Zr loading, indicative of the influence of Zr loading on the integrity of the mesoporous structure.

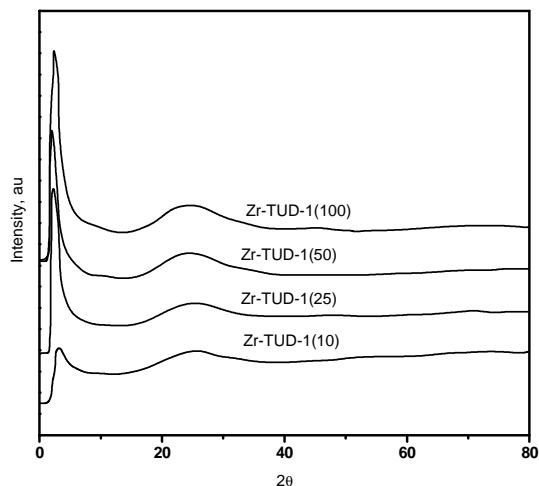


Figure 6. X-ray diffraction patterns of Zr-TUD-1 samples

The absence of zirconia crystals in the XRD-spectrum of the same sample indicates that the concentration of these nanoparticles must be low. The elemental analysis (ICP-AES) and porosity measurements obtained from N₂ adsorption studies at 77 K are listed in Table 2. Elemental analysis indicated that the Si/Zr ratios in the calcined samples were the same as those in the initial synthesis gel.

Table 2. Porosity and compositional Properties of Zr-TUD-1

Sample	BET Surface area (m ² /g)	Total Pore Volume (mL/g)	Average Pore Diameter (Å)	Si:Zr
Ce-TUD-1(10)	660	0.6	20	11.0
Ce-TUD-1(25)	750	1.2	88	21.2
Ce-TUD-1(50)	770	1.3	100	47.2
Ce-TUD-1(100)	750	1.02	90	99.5

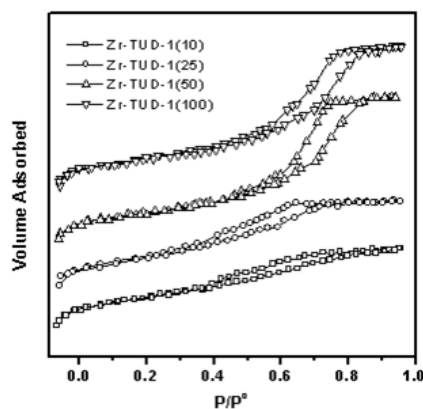


Figure 7. N₂ adsorption isotherms at 77 K recorded for zirconium-loaded TUD-1

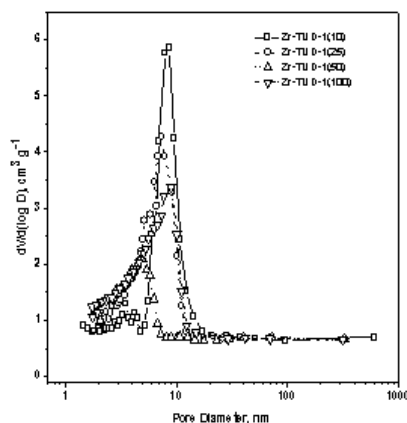


Figure 8. Pore size distribution of zirconium-loaded TUD-1 samples obtained from the N₂ adsorption data at 77K.

This excellent correlation of the Si/Zr ratio in the synthesis gel with that in the product demonstrates the high predictability of the synthesis method. This was also observed earlier for other M-TUD-1 materials.[19-21] Three samples of (Zr-TUD-1(100), Zr-TUD-1(50), and Zr-TUD-1(25)) show a type IV isotherm (Figure 9), indicated by the large uptake of nitrogen at relative pressures between 0.5 and 0.9 p/p₀ (due to capillary condensation in the mesopores). These samples also show a plateau at relative pressures above 0.9 p/p₀, indicate the absence of large mesopores, macropores or surface roughness in the measurable range (20 nm to approximately 500 nm). Additionally, these samples have a larger pore size when compared to the all silica TUD-1 (ca. 4 nm). Presumably, this is due to the presence of the large

zirconium atoms in the framework. The presence of some percolation or networking effects can also be deduced from a non-parallel adsorption and desorption isotherm.

Zr-TUD-1(10), on the other hand, showed an uptake of nitrogen at a relative pressure of up to approximately 0.5 p/p^0 and no adsorption is observed above this point. This implies the absence of large mesopores or macropores or surface roughness in the measurable range. Since pore filling occurs below the critical pressure of 0.43 p/p^0 , no hysteresis was observed. This sample displayed very little mesoporosity and a maximum pore-size distribution below 2 nm. As a result of this, the pore volume is much lower than in the other three Zr-TUD-1 samples; however, the surface area of Zr-TUD-1 (10) is comparable with the other three Zr-TUD-1 samples. The presumption that the large Zr-atom would cause an increase in pore size is not observed at this high concentration of zirconium. Instead, a differently structured material was formed with relatively small pores. This difference might be due to intensified interaction of the individual Zr atoms in the structure or due to the nanoparticles of zirconium oxide.

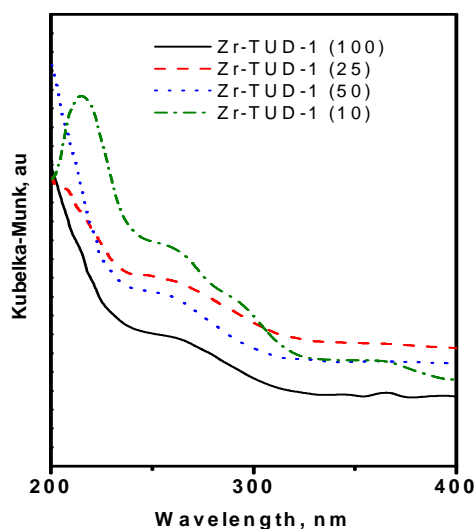


Figure 9. The UV-Vis spectra of zirconium-loaded TUD-1 samples previously heated at 180 °C for 24 h.

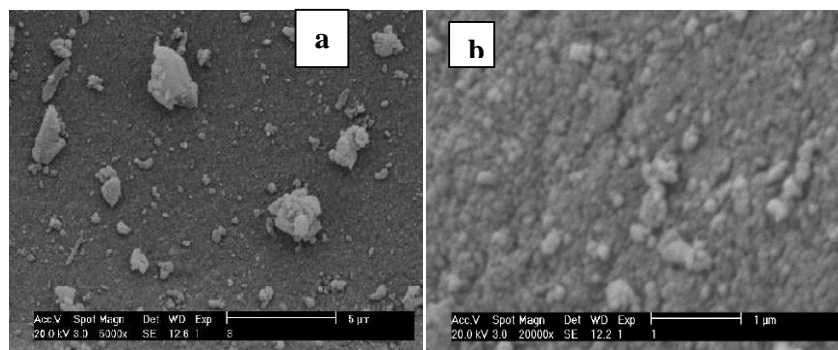


Figure 10. SEM micrograph of Zr-TUD-1 material, (a) Zr-TUD-1 (10) and (b) Zr-TUD-1 (100).

Scanning electron micrograph of Zr-TUD-1 materials did not reveal any structural indication of the material. The SEM images of Zirconium-loaded TUD-1 are presented in Figure 10. The image shows that the particles do not have any well-defined morphology. In general, the samples consist of about 5-15 μm irregularly-shaped particles. The SEM image is in line with the images of Au/Ti-TUD-1 sample presented by Haruta et al [17]. However, at high metal loading samples, the metal TUD-1 structure is changed to less uniform structures, than the low metal loading samples. This indicates the influence of a high metal concentration on the TUD-1 structure.

Catalytic activity of Metal-loaded TUD-1 catalysts:

Figures 11 and 12 compare the catalytic activities of ceria and zirconia-loaded TUD-1, respectively. The figures clearly show that DMC yields significantly improved by loading of these metal oxides onto the structure of TUD-1 framework when compared to the 2-D MCM-41.

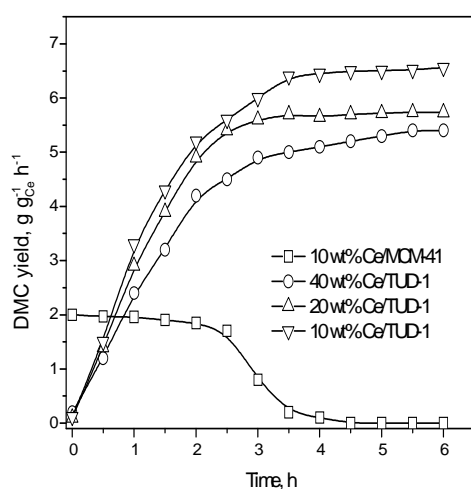


Figure 11. Catalytic activity of Ce-TUD-1 catalysts in comparison to Ce-MCM-41 catalyst

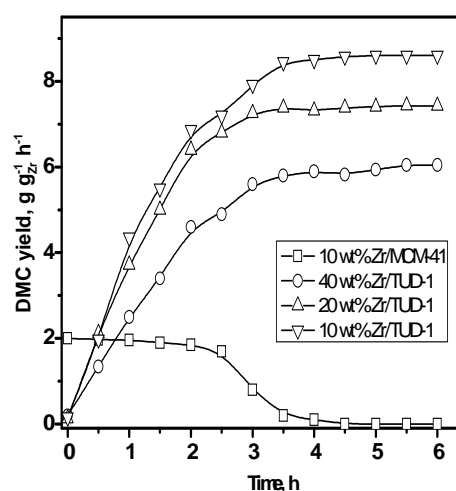


Figure 12. Catalytic activity of Zr-TUD-1 catalysts in comparison to Ce-MCM-41 catalyst.

Apparently, loading with 10% metal oxide seems to be ideal for this reaction. Most probably larger clusters of metal oxides would be formed at higher loadings of the metal oxide.

However, much better performance of catalysts containing mixtures of both ceria and zirconia could be observed as depicted in Figure 13 and 14. These results indicate a synergistic effect of both ceria and zirconia on the catalytic activity for both catalyst as it will be further explained in the near future.

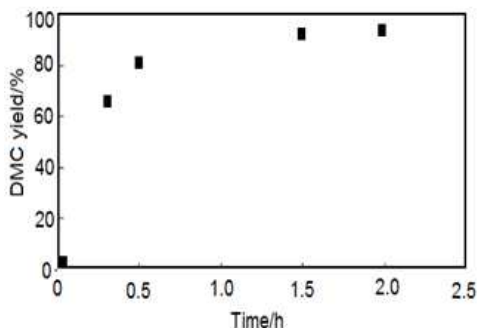


Figure 13. DMC Yield as a function of reaction time using 1.0 CeO-ZrO₂-TUD-1 Catalysts.

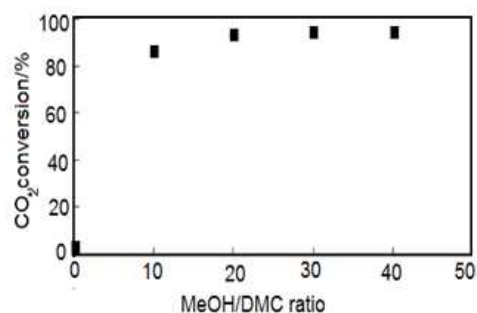


Figure 14. CO₂ conversion as a function of methanol/DMC ratio using 1.0 CeO-ZrO₂-TUD-1 Catalysts.

Acknowledgements:

The authors strongly appreciate the Deanship of Scientific Research, King Abdulaziz University for funding Project 112/28.

References

- [1] Delledonne, D.; Rivetti, F.; Romano, U., *Applied Catalysis A: General* 2001, 221, (1-2), 241.
- [2] Anderson, S.A.; Root, T.W., *Journal of Molecular Catalysis A: Chemical* 2004, 220, (2), 247.
- [3] Anderson, S.A.; Root, T.W., *Journal of Catalysis* 2003, 217, (2), 396.
- [4] Shaikh, A.A.G.; Sivaram, *Chem. Rev.* 1996, 96, 951-976.
- [5] Parrish, J.P.; Salvatore, R.N.; Jung, K.W., *Tetrahedron* 2000, 56, 8207-8237.
- [6] Tundo, P.; Selva, M., *Accounts of Chemical Research* 2002, 35, (9), 706.
- [7] Ono, Y., *Applied Catalysis A: General* 1997, 155, (2), 133.
- [8] Jansen, J.C.; Shan, Z.; Marchese, L.; Zhou, W.; Puil, N.V.D.; Maschmeyer, T., *Chemical Communications* 2001, (8), 713.
- [9] Behrsing, T.; Bond, A.M.; Deacon, G.B.; Forsyth, C.M.; Forsyth, M.; Kamble, K.J.; Skelton, B.W.; White, A.H., *Inorganic Chim. Acta* 2003, 352, 229.
- [10] Ramanathan, A.; Klomp, D.; Peters, J.A.; Hanefeld, U., *Journal of Molecular Catalysis A: Chemical* 2006, 260, (1-2), 62.
- [11] Barret, E.P.; Joyner, L.G.; Halenda, P.H., *J. Am. Chem. Soc.* 1951, 73, 373.
- [12] Lippens, B.C.; Boer, J.H.d., *Journal of Catalysis* 1965, 4, 319.
- [13] Sing, K.S.W.; Everett, D.H.; Haul, R.A.W.; Moscou, L.; Pierotti, R.A.; Rouquerol, J.; Siemieniewska, T., *Pure Appl. Chem.* 1985, 57, (4), 603.
- [14] Hamdy, M.S.; Mul, G.; Wei, W.; Anand, R.; Hanefeld, U.; Jansen, J.C.; Moulijn, J.A., *Catalysis Today* 2005, 110, (3-4), 264.
- [15] Bensalem, A.; Bozon-Verduraz, F.; Delamar, M.; Bugli, G., *Appl. Catal. A: Gen* 1995, 121, 81.
- [16] Zaki, M.I.; G.A.M. Hussein; Mansour, S.A.A.; Ismail, H.M.; Mekhemer, G.A.H., *Colloids Surfaces A: Physicochem. Eng. Aspects* 1997, 127, 47.

- [17] Sinha, A.K.; Seelan, S.; Okumura, M.; Akita, T.; Tsubota, S.; Haruta, M., *Journal of Physical Chemistry B* 2005, 109, (9), 3956.
- [18] Hamdy, M.S.; Ramanathan, A.; Maschmeyer, T.; Hanefeld, U.; Jansen, J.C., *Chemistry - A European Journal* 2006, 12, (6), 1782.
- [19] Anand, R.; Hamdy, M.S.; Hanefeld, U.; Maschmeyer, T., *Catalysis Letters* 2004, 95, (3-4), 113.
- [20] Hamdy, M.S.; Mul, G.; Jansen, J.C.; Ebaid, A.; Shan, Z.; Overweg, A.R.; Maschmeyer, T., *Catalysis Today* 2005, 100, (3-4), 255.
- [21] Hamdy, M.S.; Berg, O.; Jansen, J.C.; Maschmeyer, T.; Moulijn, J.A.; Mul, G., *Chemistry - A European Journal* 2006, 12, (2), 620.